

Inter-filament Attraction Narrows the Length Distribution of Actin Filaments

David Biron¹, Elisha Moses¹, Itamar Bonukhov², and S. A. Safran²¹Departments of Physics of Complex Systems and Materials and Interfaces², Weizmann Institute of Science
(Dated: December 23, 2021)

We show that the exponential length distribution that is typical of actin filaments under physiological conditions dramatically narrows in the presence of (i) crosslinker proteins (ii) polyvalent counterions or (iii) depletion mediated attractions. A simple theoretical model shows that in equilibrium, short-range attractions enhance the tendency of filaments to align parallel to each other, eventually leading to an increase in the average filament length and a decrease in the relative width of the distribution of filament lengths.

PACS numbers: xx.xx

Introduction

The protein actin in its filamentous form (F-actin) is a major structural component in the cytoskeleton network, and plays an active role in maintaining the leading edge of moving cells [1]. In all these structures, the filaments are dynamic objects that continuously polymerize and depolymerize as part of their normal function. The physical properties of the overall structure (mechanical strength, viscoelastic response, etc.) depend on the properties of the filaments that form the structure and, in particular, on their length distribution.

In vitro experiments on F-actin under physiological conditions (with and without capping proteins) reveal a wide, exponential distribution of lengths [2, 3, 4]. This can be attributed theoretically to the fact that the underlying (dominant) stochastic dynamics, namely monomer exchange, is an "homogeneous zero range process" (ZRP) [5] which generates an exponential steady state distribution. At the same time, equilibrium theories of self-assembly of polymers or micelles predict an exponential distribution determined by the competition of the end-

cap energy and the translational entropy [15]. Indeed, nucleating and severing proteins such as gelsolin [6] are known to modify the average filament length, $\langle l \rangle$, but not the coefficient of variance of the length distribution σ^2/l^2 , where σ is the standard deviation of the distribution.

In contrast, we have recently observed that when crosslinker proteins are added to an F-actin solution they enhance the preference for overlapping filament sections. As a result, the shape of the distribution changes and σ is reduced approximately by half [7]. Similar behavior is also observed in the presence of myosin aggregate [8].

In this letter, we argue that the narrowing of the length distribution is a general effect arising from short-range attraction between the filaments; chemically crosslinking is not necessary to observe the reduction in σ . Specifically, we show experimentally that both depletion mediated attractions in a solution containing inert polymers (PEG), and electrostatic interactions induced by multivalent counterions (spermine) result in attractions that significantly narrow the distribution. A simple theoretical approach demonstrates that this effect should be observed for any mechanism that leads to short-ranged attraction. The attractions increase the tendency of filaments to lie parallel to each other and to grow concurrently. As a result, the shape of the length distribution changes dramatically: from a monotonously decreasing exponential distribution, to a non-monotonous Gaussian-like distribution with a well-defined peak at large filament lengths. Generally speaking, exponential distributions where the width scales as the average, are typical of systems where entropy dominates over interaction energies; Gaussian-like distributions, where the width is much smaller than the average, are typical of systems where interaction energies dominate.

Confronting experimental measurements for the values of the elastic constants of the actin gel have been suggested to be a result of variations in the length distribution of F-actin [9]. Furthermore, cells provide a biochemical environment crowded with macromolecules. Crowding leads to depletion mediated attractions that can be reproduced in vitro by adding inert polymers such as polyethylene glycol (PEG) [10]. We therefore suggest that the physical effects described in this study have a

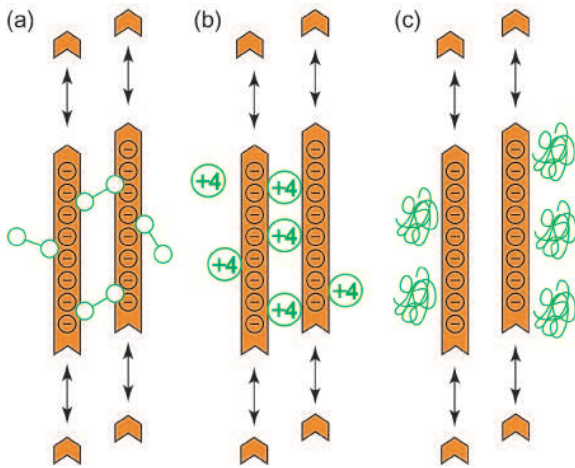


FIG. 1: A schematic view of three different attraction agents ("linkers") and their effect on actin polymerization: (a) crosslinker proteins (b) polyvalent counterions, and (c) inert polymers giving rise to depletion mediated attractions.

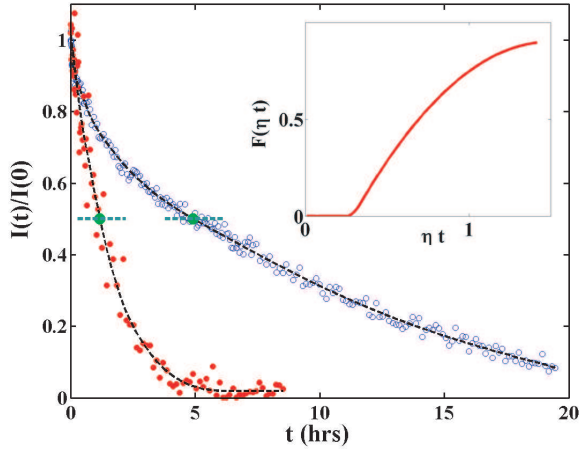


FIG. 2: Normalized fluorescence data from an actin depolymerization measurement. The full circles denote F-actin which was incubated in the presence of 100mM spermine and depolymerized by diluting the solution 10-fold with 0.4X AP-buffer. Empty circles denote a control measurement where the F-actin solution (without spermine) was diluted with a buffer containing 10mM spermine. The dashed curves show the non-parametric fits to the data and the straight lines are drawn where the intensity of fluorescence reaches half of its initial value. Inset: an example of a cumulative distribution functions of filament lengths which was extracted from the data. The depolymerization rate, τ , is normalized as explained in [7].

role in regulating the properties of actin gels in cells and in tissues.

Experimental materials and methods

Spermine (4 HCl) and PEG (MW = 6000) were purchased from Sigma-Aldrich Ltd. (Rehovot, Israel). Pyrene labelled actin (10% labelled monomers) was purchased in lyophilized form from Cytoskeleton Inc. (Denver CO, USA) and polymerized at a stock concentration of 0.15mg/ml in 0.4X polymerization buffer with 0.5mM ATP ("AP-buffer") as described in [7]. G-actin aliquots were quick frozen in liquid N_2 , and pre-spun at 150000g, 4°C, for 2 hours upon thawing. After polymerization, equilibrated spermine (100mM) or PEG (4% w/w) were added to the F-actin solution from 10X stocks (diluted in AP-buffer) and an equal volume of buffer was added to control F-actin aliquots. The filaments were then incubated for at least two hours at room temperature before performing a depolymerization assay.

Depolymerization was induced by diluting the F-actin solution 10-fold using a cut pipette tip. F-actin aliquots incubated with PEG (spermine) were compared to control filaments depolymerized in AP-buffer containing 0.4% PEG (10mM spermine). Depolymerization was monitored with a Spex FluoroLog-3 spectrofluorometer, Jobin Yvon Ltd. (London) at 20°C, while stirring very gently to avoid filament breaking. An OD 1 ND filter

Incubation	Dilution	r	$\tau_{1=2}$ (hr)
{	2% -actinin	1.6 0.2 [7]	1.5 0.4 [7]
20% -actinin	{	1.0 0.2 [7]	0.5 0.2 [7]
{	0.4% PEG	1.9 0.2	1.5 0.4
4% PEG	{	1.1 0.2	0.5 0.2
{	10mM spermine	1.2 0.3	5.5 1.5
100mM spermine	{	0.5 0.2	1.2 0.5

TABLE I: Results from depolymerization measurements under four different sets of conditions. The "incubation" ("dilution") column specifies what was added to the 0.4X AP-buffer during the incubation (dilution) of the actin filaments. The values for the coefficients of variance and the depolymerization half-times given in each case are averaged over 4-6 experiments for each set of conditions and the errors are statistical.

was used to minimize photobleaching. Photobleaching was measured separately and corrected for when found to be significant. The data was non-parametrically fitted to a smooth, monotonically decreasing and convex curve. τ was then derived from the smooth curve as described in [7].

Experimental results

Fig. 2 presents data from an actin depolymerization assay in the absence and in the presence of spermine ions. We analyzed 5 depolymerization experiments after incubation with spermine ions, 4 spermine control depolymerizations, 6 depolymerization experiments after incubation with PEG and 6 PEG control depolymerizations (as described in Sec. II). The values extracted for r and $\tau_{1=2}$ are summarized in Table 1. In both cases, r was about 2-fold smaller and $\tau_{1=2}$ was about 3-fold smaller as compared with the control depolymerization measurements. These results are consistent with results obtained for crosslinked filaments [7]. When the length distribution is narrower the depolymerization process is more efficient since the dominant portion of the filament length distribution depolymerizes concurrently, resulting in smaller values of $\tau_{1=2}$. As explained below, narrow length distributions are a signature of attractive inter-filament interactions, whether they result from depletion forces [11] or from multivalent counterions [12]; physical crosslinking is not a necessity.

The average amplitude of the fluctuations around the smooth fit to the depolymerization curve was similar for dilution buffer containing 10mM spermine and not containing spermine. However, the presence of 0.4% PEG in the dilution buffer introduced a noise amplitude approximately twice as large. The effect of noise is more pronounced at the late stages of the measurement resulting in an apparent longer tail of the distribution of lengths, which leads to an artificially larger value of r (see [7]). This is reflected in the fact that the value of r in the well established case of the exponential length distribution of pure F-actin was larger than unity when

extracted from dilution in the presence of PEG. It is important to note that despite this effect, an unambiguous decrease of both r and $\langle l \rangle_{l=2}$ is preserved. This indicates that the interaction does indeed reduce the variance of the lengths.

Theory

Actin polymerization is a dynamic process and most theories that address filament length distributions [4, 13, 14] are based on kinetic equations for the various processes involved (e.g., monomer association, dissociation etc.). On the other hand, Flory has already noted [13] that quite often, kinetic arguments leading to a steady state distribution can be replaced by equilibrium arguments. In particular, the presence of actin-severing proteins (gel-solin, cofilin, ...) ensures that the filament distribution follows the equilibrium distribution and does not depend on dynamic instabilities. Indeed, the exponential distribution that is typical of F-actin is also found in self-assembling systems where surfactant molecules form linear micelles and equilibrium is maintained through exchange of surfactant molecules with the solution [15]. The equilibrium approach has the advantage that it provides a natural framework to systematically study the effect of inter-filament interactions.

The theoretical starting point is the following free energy (per unit volume) of a solution consisting of concentrations, ρ_l , of filaments of lengths $l = 1; 2; 3; \dots$:

$$f = \sum_l \rho_l [\ln(\rho_l v_0) - 1 + \frac{1}{l} + b] + \sum_{l < l'} w(l; l') \rho_l \rho_{l'} \quad (1)$$

The logarithmic term represents the translational entropy of the filaments where v_0 is a monomer volume. Here and in the following, all energies are in units of the thermal energy $k_B T$. The energy of a single filament consists of a term linear in l which is due to the interaction between neighboring monomers and an l -independent term that is basically the end-cap energy, b , of the filaments. The next term is the two-body interaction term where $w(l; l') = \int d\mathbf{r} d\Omega \exp(-\frac{u_0}{2} \frac{r}{l} \frac{r'}{l'})$ is the second virial coefficient of a pair of rods of lengths $l; l'$ averaged over their mutual separation r and angle [16]. Finally, the Lagrange multiplier is added to free energy to fix the total monomer concentration $\sum_l l \rho_l = \rho_m$.

The equilibrium length distribution is obtained by minimizing the free energy with respect to ρ_l :

$$\rho_l = \rho_0 \exp \left(-a l - \sum_{l'} w(l; l') \rho_{l'} \right) \quad (2)$$

where $\rho_0 = \exp(-b)/v_0$ and $a = \frac{1}{\rho_0}$. In the absence of inter-filament interactions, the distribution $\rho_l^{(0)}$ is exponential with an average filament length $\langle l \rangle_{l=1} = 1/a = (\rho_m = \rho_0)^{-1/2}$ and $r = 1$. Note, that because of monomer

conservation the value of ρ_0 does not affect the length distribution and only shifts the monomer chemical potential by a constant.

The leading contributions to the virial coefficient due to hard-core repulsions are $w_{HC}(l; l') = (\frac{1}{2} - 1) l l' d + \frac{1}{2} (1 + l' - l)^2 d^2$ where $d = l; l'$ is the filament diameter [17]. As noted by Ben-Shaul and Gelbart [17], the first term merely shifts the monomer chemical potential by a constant and has no effect on the distribution. The next term is equivalent to a reduction in ρ_0 and leads to an increase in the average filament length [17] while the distribution remains exponential with $r = 1$.

This is no longer the case when linker-mediated inter-filament attractions are introduced [8]. The new contribution reads

$$w_{att}(l; l') = -\frac{1}{2} l l' (1 - e^{u_0}) + 2 d \left(\frac{1}{2} l_1 - 1 + \frac{e^z}{z} \right) + (l_2 - \frac{1}{2} l_1) (1 - e^z) \quad (3)$$

where $u_0 < 0$ is the linker-mediated short-range attraction per monomer and z is the range of the attraction. The first term is the contribution from configurations where the filaments cross at large angles while the second term is the contribution from parallel configurations with $z = (\frac{1}{2} - d)u_0$, $l_1 = \min(l; l')$, and $l_2 = \max(l; l')$. The latter is divided into a term independent of l_2 due to configurations where the two rods overlap only partially and configurations where the short filament is fully adjacent to the long filament.

Eqs. 2,3 allow one to determine the length distribution f_l . In order to simplify the calculation we look for a perturbative solution around the noninteracting distribution of the form $\rho_l = \rho_l^{(0)} (1 + \rho_l^{(1)})$ where $\rho_l^{(1)} \ll 1$. To leading order, the solution is then

$$\rho_l = \exp(-a l) \sum_{l'} w(l; l') \rho_{l'}^{(0)} \quad (4)$$

where a is determined from the conservation constraint $\sum_l l \rho_l^{(0)} = \rho_m$.

Typical solutions for the normalized length distribution $P_l = \rho_l / \rho_0$ and the accumulated distribution $F_l = \sum_{l'=1}^l P_{l'}$ for different values of the attraction strength, u_0 , are shown in Fig. 3. The solutions for $u_0 = 0.001$ generally agree with the measured distributions (see inset in Fig. 2) except for the short filament end, which is beyond the resolution of the experiment. As the attraction becomes stronger, the distribution develops a peak at longer and longer filament lengths and with increasing magnitude. Since u_0 is defined as the interaction energy per monomer, it is the magnitude of $l u_0$ that determines whether the inter-filament interactions are strong enough to modify the distribution.

The effect on the coefficient of variance r is non-monotonic as shown in Fig. 4b. At first, the ratio increases above one but soon it reaches a maximum and

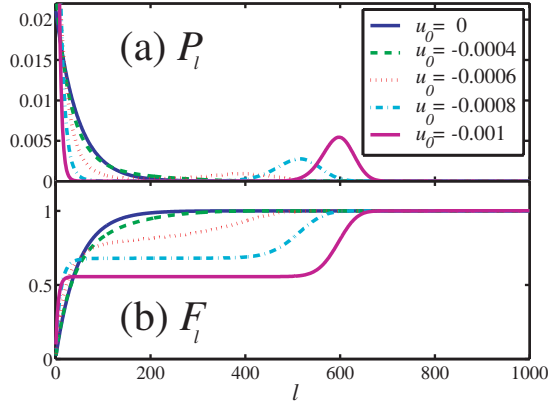


FIG. 3: Length distributions p_l (a) and accumulated distributions F_l (b) for different values of the attraction strength j_{0j} (in units of $k_B T$). The values used in the calculation are $\mu_m = 0.1$, $\mu_0 = \exp(10)$, $\sigma = 1$, $d = 1/2$ and the cutoff value for the filament length is $l_{\max} = 1000$.

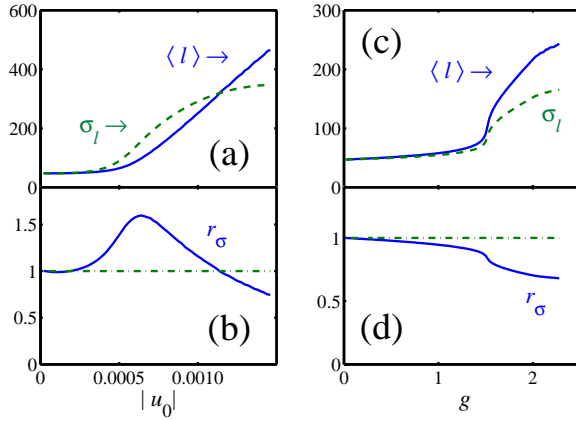


FIG. 4: Average filament length $\langle l \rangle$ and root mean square σ_l (a) and their ratio r_σ (b) as functions of the attraction strength j_{0j} within the perturbative approximation. The results of the mean field approximation are shown in (c) and (d) where the horizontal axis is $g = u_0^2$. Same physical values as in Fig. 3.

decreases below one. The initial increase in r_σ is due to the bimodal length distribution at intermediate values of u_0 , and the consequent decrease occurs when the longer filaments dominate the length distribution.

Because of the perturbative nature of the approximation, it can not correctly describe the behavior in the presence of strong attractions. In this limit, of strong

interactions, the behavior can be studied within a mean field-like approximation where the main assumption is that the sum in the exponent of Eq. 2 is dominated by the "typical" filament length $l = \langle l \rangle$. It is helpful to expand the attraction term $w(l; l')$ in powers of u_0 and neglect a term proportional to l^3 that is only significant in the immediate vicinity of l . The length distribution is then of the form

$$P_l = \frac{1}{Z} \left(\frac{e^{a + g l^2}}{e^{a + g l^2}} \right)^{l^2} \frac{1}{l} \quad (5)$$

where $g = u_0^2$. It is now apparent from Eq. 5 that while the length distribution of long filaments ($l \gg 1$) remains exponential, that of short filaments ($l \ll 1$) shows two local maxima, first at $l = 0$ and then at $l = 1$. Furthermore, while for small values of j_{0j} the distribution reduces to the original exponential one, at large values of j_{0j} the distribution shows a narrow peak at $l = 1$. With three unknowns a, l, σ , the distribution function, P_l , can be calculated by solving the following three equations: (i) the monomer conservation condition $\sum_l l P_l = \mu_m$, (ii) the consistency condition $\sigma = \mu_0 \exp(a + g l^2)$, and (iii) the condition that $\langle l \rangle = 1$. As shown in Fig. 4, the results of this calculation (valid only at large values of j_{0j}) qualitatively confirm the results of the perturbative approach.

Conclusions

In summary, we have shown that in the presence of short-ranged attractions the coefficient of variance of the length distribution of F-actin is decreased due to an increasing tendency of the filaments to align parallel to each other even without chemical crosslinking. The phenomena is quite general and does not depend on the exact details of the attraction mechanism: the attractions can be induced by multivalent counterions or can be electrostatic by nature; they can occur in a crowded environment like the cell as a result of depletion mediated attractions; or they can be induced by linker proteins, which attach actin filaments to each other in the cytoskeleton and in other filament aggregates.

Acknowledgments: We would like to thank Oleg Krivevsky for access to equipment and Nir Gov for useful discussions. Partial support from the German-Israeli Foundation and the Israeli Science Foundation is gratefully acknowledged.

[1] See, e.g., Lodish, H. et al (2000) Molecular Cell Biology, (4th edition, W. H. Freeman, New York).
 [2] J. Xu, J. F. Casella and T. D. Pollard, Cell Motil. Cytoskeleton 42, 73 (1999).
 [3] R. Littlefield and V. M. Fowler, Annu. Rev. Cell Dev.

Biol. 14 487 (1998).
 [4] L. Edelstein-Keshet and G. B. Ermentrout, Bull. Math. Biol. 60, 449 (1998).
 [5] M. R. Evans, Braz. J. Phys. 30, 42 (2000).
 [6] See, e.g., H. L. Yin, Gelsolin in Guidebook to the Cy-

- toskeletal and Motor Proteins, 2nd ed., edited by T. Kreis, R. Vale (Oxford University Press Inc., New York, 1999) pp. 99-102 and other sections as well.
- [7] D. Biron and E. Moses, *Biophys. J.* **86**, 3284 (2004).
- [8] M. Kawamura and K. Maruyama, *J. Biochem.* **67**, 437 (1970).
- [9] J. Xu et al., *Biophys. J.* **74** 2731 (1998).
- [10] See, e.g., M. Hoesek and J. X. Tang, cond-m at/0309674 and references therein.
- [11] A. Suzuki, M. Yamazaki and T. Ito, *Biochem.* **35**, 5238 (1996).
- [12] T. Angelini, H. Liang, W. Wriggers, and G. C. L. Wong, *Proc. Nat. Acad. Sci.* **100**, 8634 (2003).
- [13] P. J. Flory, *Principles of Polymer Chemistry* (Cornell University Press, Ithaca 1953), Chapter 8.
- [14] F. Oosawa and M. Kasai, *Mol. Biol.* **4**, 10 (1962).
- [15] S. A. Safran, *Statistical Thermodynamics of Surfaces, Interfaces, and Membranes* (Addison-Wesley, Reading 1994).
- [16] L. Onsager, *Ann. N.Y. Acad. Sci.* **51**, 627 (1949).
- [17] A. Ben-Shaul and W. M. Gelbart, *J. Phys. Chem.* **86**, 316 (1982); W. M. Gelbart, A. Ben-Shaul, W. E. McMullen and A. Masters, *J. Phys. Chem.* **88**, 861 (1984).
- [18] The calculation follows closely the lines of the Onsager theory [16]. See, e.g., I. Borukhov, R. F. Bruinsma, W. M. Gelbart and A. J. Liu, (in preparation).